



## Facile fabrication of sulfamic acid / Al-MIL-53 for Congo red removal

Awad I. Ahmed, Ossama Elbanna, Alzahraa Mohamed

Chemistry Department, Faculty of Science, Mansoura University, Mansoura, Egypt

Received: 9/9/2019  
Accepted: 20/10/2019

**Abstract:** Solvothermal method was used for preparation of AL-MIL-53 MOF and modified by different amounts of sulfamic acid (SA= 15, 25, 30, 50, and 60%) by impregnation method. MOFs were characterized by Fourier transform infrared spectrometry. This technique confirmed successful loading of sulfamic acid onto Al-MIL-53. The prepared samples were applied to the adsorption of Congo red dye (CR) from wastewater. The amount of adsorption increases by increasing amount of SA till reaches to 25%SA/MIL-53. After this percent of SA, the amount of adsorption decreases. It was obvious that the best adsorption occurs at pH=2. The isotherms and kinetics data were represented by Langmuir adsorption isotherm and pseudo 2nd order kinetic model.

**keywords:** MOFs, Al-MIL-53, sulfamic acid, Adsorption, Congo red

### 1. Introduction

Metal organic frameworks (MOFs) consist of interaction between metal ions and organic ligands to form different dimensional framework [1–3]. Omar Yaghi synthesized the first MOFs in the mid-1990 and start to develop a compound which could be designed with a variety of metal ions and organic compounds [4–5]. MOFs attract attention due to their unusual and unique properties and structure. MOFs are crystalline, porous, large surface area, and has many structures [6,7]. MOFs were used in various application such as adsorption [8–10], separation [9,10] sensing [13], catalysis [14], and proton conduction [15], as well as photocatalysis [16], and biocatalysis [17]. Room temperature [4], solvothermal, hydrothermal [18], electrochemical (EC) [19], microwave (MW) irradiation and ultrasonication methods [20] are used for preparation of MOFs.

Aluminium (III) terephthalate (AL-MIL-53) exhibits exceptional structural stability in aqueous solution [21], high thermal stability, low-cost and available raw materials. MOFs have the relatively high surface area and also has ability to resistant moisture [22]. MOFs can be modified by the addition of heteropoly acid, mineral acid or metal nanoparticles through different methods [23]. Sulfamic acid (SA,  $H_2NSO_3H$ ) is an example of inorganic acid which has mild acidity. SA has various

properties such as non-volatile, noncorrosive, and physical stability. It has no solubility in organic solvents and has zwitter ion property when existing in the form of solid state [23, 24].

Contamination of water caused by dyes and heavy metal attract great interest due to their harmful effect. Many organisms and marine communicates are exposed to poison effect from this contamination [25]. There are different methods for removing contamination biologically, chemically and physically. In biological methods, many organic compounds are degraded using microbial degradation. A chemical method such as coagulation and flocculation [26] and adsorption [27]. A physical method such as membrane separation [28] and adsorption. Adsorption is the most effective way due to its cheap price and simple design. It is also operated easily [29]. Congo red (CR) is an example of anionic dye which has many applications in industries such as printing, dyeing, rubber and etc. [30]. CR also has effect on clotting of blood and may lead to problems in respiratory system [31]. So it is very important to remove CR.

In this search, AL-MIL-53 was prepared by solvothermal method and different amount of sulfamic acid was added by using the impregnation method and characterized by FT-

IR .The prepared samples were applied as an adsorbent for removal of CR. The effects of pH, time, adsorbent dose and initial concentration were studied .The parameters of adsorption isotherms and adsorption kinetics were also determined.

## 2. Experimental

### 2.1 Materials

All starting materials and solvents applied in this study were used are available: aluminium (III) chloride [ALCl<sub>3</sub>, 98%, ALPHA], 1,4 benzenedicarboxylic acid (known as terephthalic acid, C<sub>8</sub>H<sub>6</sub>O<sub>4</sub>, 98%, ALPHA ) and N,N-dimethyl formamide (known as DMF, (CH<sub>3</sub>)<sub>2</sub>N-CHO, 99.5%, ADWIC), sulfamic acid [H<sub>3</sub>NSO<sub>3</sub>, 98.5%], and Ethanol [C<sub>2</sub>H<sub>5</sub>OH, ≥99.5%, ALAMIA].

### 2.2. Preparation of AL-MIL-53

The AL-MIL-53 was prepared by a solvothermal method as reported [32]. A mixture of ALCL<sub>3</sub> (2 mmol, 532 mg), 1, 4 benzene dicarboxylic acid (1mmol, 332 mg) and 35ml DMF was sonicated and stirred for 30 min. The mixture was put into a Teflon-lined autoclave bomb and put in an oven for 24 h at 150°C. The suspension left to cool then was centrifuged and washed with DMF to remove excess of terephthalic acid encapsulated inside pores then dried at 100 °C overnight.

### 2.3. Synthesis of wt% sulfamic acid/AL-MIL-53.

Sulfamic acid (SA) was added onto AL-MIL-53 by impregnation method. 1gm of AL-MIL-53 in 20ml ethanol was sonicated and mixed with the calculated amount of SA in 10 ml ethanol under vigorous stirring then made was refluxed at 100 °C for 24 hrs. Then, the product was washed with ethanol and dried in 100°C overnight. The amounts of sulfamic acid were added to get (15, 25, 30, 40, 50 and 60 wt %) SA-MIL-53.

### 2.4. Adsorption of Congo red.

AL-MIL-53 and SA-AL-MIL-53 were carried out for adsorption of Congo red. 0.05gm of sample was added to 50 ml solution of the dye with different initial concentration ranged from 50 to 300 mg L<sup>-1</sup> (ppm). 0.1M HCl or 0.1M NaOH was used for adjusting the pH. The bottles were shaken for the required adsorption time. The equilibrium concentrations of Congo

red were measured by using spectrophotometer ( $\lambda_{\max}$  =497nm).

## 3. Results and discussion

### 3.1. FT-IR analysis

FT-IR of all prepared samples were analysed by using FT-IR spectroscopic technique on Nicolet magna-IR 550 spectrometer with 128 scans and 4cm<sup>-1</sup> resolution in the mid-IR region ranged from 400-4000 cm<sup>-1</sup>. FT-IR spectra of the prepared AL-MIL-53 and SA-AL-MIL-53 are shown in Fig.1. The spectra display characteristic peak in the range of 1400-1700 cm<sup>-1</sup> indicating the vibration of (C=C) of the aromatic ring. Also, asymmetric stretching vibration of -COOH appears at bands 1511 and 1600 cm<sup>-1</sup> whereas 1416 cm<sup>-1</sup> and 1438 cm<sup>-1</sup> bands are due to symmetric stretching of -COOH. The bands appeared in 1276 cm<sup>-1</sup> and 1131 cm<sup>-1</sup> for all the samples are related to C-O vibration [33]. Whereas, the broad band at 730-1100 cm<sup>-1</sup> is related to stretching vibration of C-H in aromatic ring and band at 1023 cm<sup>-1</sup> corresponds to the presence C-O-AL [34]. A broad band around 3450 cm<sup>-1</sup> is due to the stretching vibration of O-H from water or carboxylic group and also the band appears at 478 cm<sup>-1</sup> related to AL-O in the Al-MIL-53 [35-36]. The bands around 3660 cm<sup>-1</sup> and 995 cm<sup>-1</sup> are due to the symmetric and asymmetric stretching of the hydroxyl groups of AlO<sub>4</sub>(OH)<sub>2</sub> [37]. The broad band which appears in the range of 3000-3500 cm<sup>-1</sup> is due to N-H vibration. The weak band appears in 2800 cm<sup>-1</sup> is due to N-H stretching and the peak appears in 1185 cm<sup>-1</sup> is related to vibration of (O=S=O). the band at 600 cm<sup>-1</sup> is related to SO<sub>3</sub> deformation and the existence of new vibration band at 660 cm<sup>-1</sup> related to NH<sub>2</sub> vibration[38]. The peaks at 1026 and 1234 cm<sup>-1</sup> are corresponded to S-O stretching and stretching -SO<sub>3</sub>H vibration.

### 3.2 Adsorption of Congo red.

#### 3.2.1 Effect of pH.

The change in the pH has effect on the adsorption of CR as shown in Fig.2. The initial dye concentration of 100ppm and 0.05 g 25%SA-AL-MIL53 dried at 100 °C are used. From Fig.2, the amount adsorbed was almost constant 97.67 mg/g to pH=6, then the amount adsorbed decreased to 72.47 mg/g for pH= 8. At pH=2 surface with positive charge interact

with negative charge dye by strong interaction so maximum adsorption occurs. But in case of higher pH (pH=8), the surface has negative charge and repulsive with the anionic dye so the amount of adsorbed decreased [39].

### 3.2.2 Effect of amount of adsorbent

Increasing in the weight of adsorbent from 0.03g to 0.07g lead to increase in the % removal and up to 0.07 g the %removal becomes almost constant as depicted in Fig.3. The increase of the adsorption is due to increase in number of adsorption sites which available for adsorption [11] and increase in surface area of adsorbent [40].

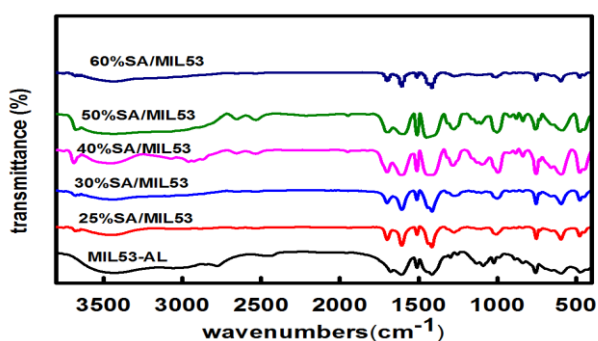


Fig.1. FT-IR of Al-MIL-53 and MIL-53 modified with sulfamic acid

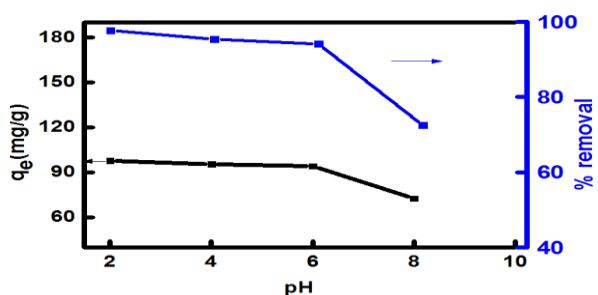


Fig.2. Effect of pH on the adsorption of CR on 25%SA-Al-MIL-53.

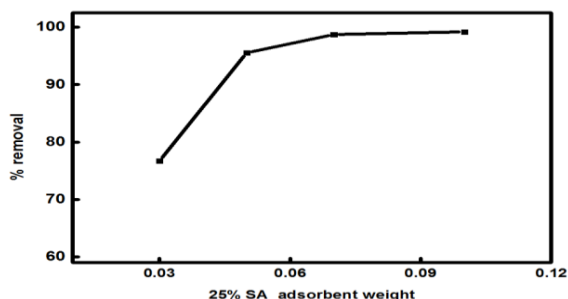


Fig.3. Effect of adsorbent dose of 25%SA-AL-MIL53 dried at 100 °C on adsorption of CR.

### 3.2.3 Adsorption Isotherms.

The adsorption isotherms indicate how CR is distributed over modified and nonmodified MIL53. Three adsorptions isotherms are

applied. Langmuir, Freundlich, and Dubinin–Radushkevich (D–R) are the most common models used to describe the adsorption mechanism. The Langmuir model applied on the homogeneous surface and when there is monolayer adsorbate on the surface of the adsorbent, The Langmuir model is given by:

$$C_e/q_e = 1/(q_{max} * K_L) + C_e/q_{max} \quad (4)$$

Where  $q_e$  (mg /g) is the amount of adsorbate adsorbed at equilibrium,  $C_e$  (mg /L) is the concentration of the adsorbate at equilibrium,  $q_{max}$  (mg/g) is the maximum amount of adsorption and  $K_L$  (L/mg) is Langmuir constants, the energy of adsorption, calculated from  $R_L = 1/ (1 + K_L C_0)$

Where  $C_0$  (mg/L) is the initial concentration of  $C_R$ . The  $R_L$  value shows the shape of the isotherm. When ( $R_L > 1$ ), the isotherm is unfavourable. The isotherm is linear when  $R_L = 1$ , also favourable adsorption when  $0 < R_L < 1$  and irreversible ( $R_L = 0$ ). Adsorption on the heterogeneous surface is the assumption of the Freundlich model and it is expressed by eqn:

$$\text{Log } q_e = \text{log } K_f + 1/n \text{ log } C_e \quad (5)$$

$K_f$  is the Freundlich constant, and  $1/n$  is the constant

associated to strength of adsorption. The value of  $n$  indicates the type of adsorption. If  $n = 1$ , the adsorption is linear. Chemical adsorption occur when  $n < 1$ . The physical adsorption is favourable when  $n > 1$ .

Physical and chemical adsorption can be differentiated by using D-R equation and its linear form is given as:

$$\ln q_e = \ln q_m - K_D \epsilon^2$$

Where  $q_e$  is the amount of CR adsorbed at equilibrium (mg/g),  $q_m$  is the theoretical adsorption amount (mg/g)  $K_D$  is a constant associated with the energy of adsorption.  $\epsilon$  is the Polanyi potential, which calculated from  $\epsilon = RT \ln (1 + 1/C_e)$  Where  $R$  is gas constant (8.314 J/mol·K),  $T$  is the temperature in Kelvin and  $C_e$  is equilibrium concentration (mg/L). The energy of adsorption calculated from the following equation:  $E = 1/\sqrt{2K_D}$

If  $E$  below 8 kJ/mol, the physical adsorption occurs. Chemical ion exchange occurs at energy between 8 and 16 kJ/mol. chemical adsorption occurs when  $E$ -values between 20 and 40 kJ/mol. The three isotherm models are

presented in Fig.4 and Table 1. These figures show that  $R^2$  obtained from Langmuir is higher than that from Freundlich and D-R and thus Langmuir is the best isotherm applied. The values of  $0 < R_L < 1$  for all adsorbent with different initial concentration  $C_0=50-200\text{ppm}$  indicated that adsorption is favorable. The values of  $E$  below  $8 \text{ kJ/mol}$  indicated that physical adsorption occurs.

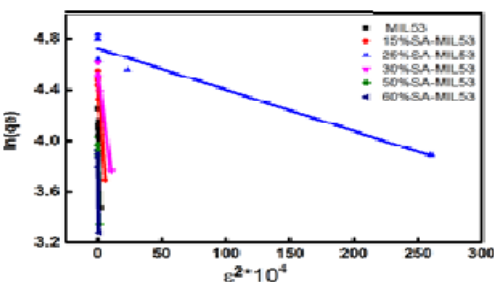
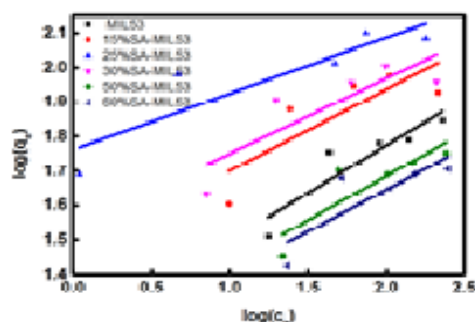
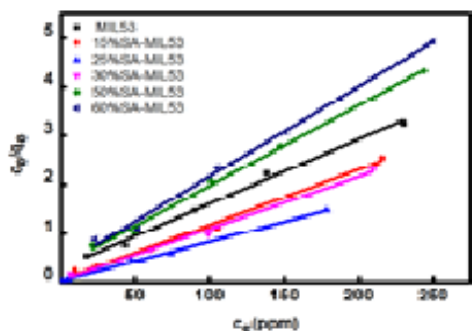


**Fig.4.** Adsorption isotherm of CR on MIL-53(Al) and different SA-Al-MIL-53 (Al).

**Table1.** Adsorption isotherms for the adsorption of CR (100ppm) with different loading content of MIL53.

Model	AL-MIL53	15%SA-Al-MIL53	25%SA-Al-MIL53	30%SA-Al-MIL53	50%SA-Al-MIL53	60%SA-Al-MIL53
<b>Langmuir</b>	$k_l=0.046$ $q_m=75.7$ $R^2=0.99$ $R_L=0.067-0.303$	$k_l=0.272$ $q_m=88.26$ $R^2=0.98$ $R_L=0.012-0.068$	$k_l=0.36$ $q_m=123.15$ $R^2=0.99$ $R_L=0.009-0.052$	$k_l=0.333$ $q_m=93.98$ $R^2=0.99$ $R_L=0.009-0.056$	$k_l=0.050$ $q_m=60.67$ $R^2=0.99$ $R_L=0.062-0.28$	$k_l=0.056$ $q_m=54.37$ $R^2=0.99$ $R_L=0.056-0.263$
<b>Freundlich</b>	$K_F=16.76$ $n=3.64$ $R^2=0.78$	$K_F=29.13$ $n=4.25$ $R^2=0.57$	$K_F=57.75$ $n=6.15$ $R^2=0.73$	$K_F=34.09$ $n=4.60$ $R^2=0.62$	$K_F=15.02$ $n=3.93$ $R^2=0.68$	$K_F=14.52$ $n=4.1$ $R^2=0.59$
<b>Dubinin-Radushkevich</b>	$K_D=3.72 \times 10^{-5}$ $q_m=64.87$ $E=115.93$ (J/mol) $R^2=0.96$	$K_D=1.4 \times 10^{-5}$ $q_m=89.37$ $E=188.98$ $R^2=0.97$	$K_D=3.2 \times 10^{-7}$ $q_m=112.97$ $E=1250$ $R^2=0.92$	$K_D=7.3 \times 10^{-6}$ $q_m=93.33$ $E=261.71$ $R^2=0.97$	$K_D=5.1 \times 10^{-5}$ $q_m=54.3$ $E=99.01$ $R^2=0.95$	$K_D=5.76 \times 10^{-5}$ $q_m=50.06$ $E=93.16$ $R^2=0.93$

### 3.2.4 Effect of contact time and kinetics of adsorption

Fig.5 shows that the amount adsorbed of CR at different contact time for AL-MIL-53 and AL-MIL-53 modified with sulfamic acid (initial dye concentration = 100 ppm, pH=2, and 0.05g adsorbent). Fig.5a. depicted that the % removal of CR was fast in the first of 30 min then increase slowly by increasing time until reach to equilibrium after 4h.

The kinetics of adsorption has been applied to know how the adsorption occurs. Pseudo-first-order, pseudo-second-order and the Elvoich equation were applied for CR adsorbed over AL-MIL-53 and modified Al-MIL-53 as

shown in Figs 5. The equation for the pseudo 1<sup>st</sup> order kinetic model is given by eqn (1):

$$\text{Log}(q_e - q_t) = \text{log } q_e - (k_1/2.303) t \quad (1)$$

Where  $q_t$  (mg /g) represents the amount adsorbed at time (t) and  $q_e$  (mg /g) is the amount adsorbed at equilibrium time and  $k_1$  ( $\text{min}^{-1}$ ) is the rate constant of the pseudo 1<sup>st</sup> order. Plotting of  $\text{Log}(q_e - q_t)$  against t to obtain the first order parameters was done. The pseudo 2nd order kinetic model is expressed by eqn (2)

$$t/q_t = 1/k_2 q_e^2 + t/q_e \quad (2)$$

Where  $k_2$  (g / (mg. min)) is the rate constant. Plotting  $t/q_t$  versus time was used to obtain pseudo 2<sup>nd</sup> order parameters. Also, The Elovich

equation model is applied and can be expressed as in eqn (3)

$$q_t = \alpha \ln \beta + \beta \ln t \quad (3)$$

Where  $\alpha$  (mg/g min) is the initial rate of adsorption and  $\beta$  (g/mg) is the desorption constant. They obtained by plotting  $q_t$  against  $\ln t$ . All the kinetic parameters and correlation coefficients ( $R^2$ ) from the kinetic models are

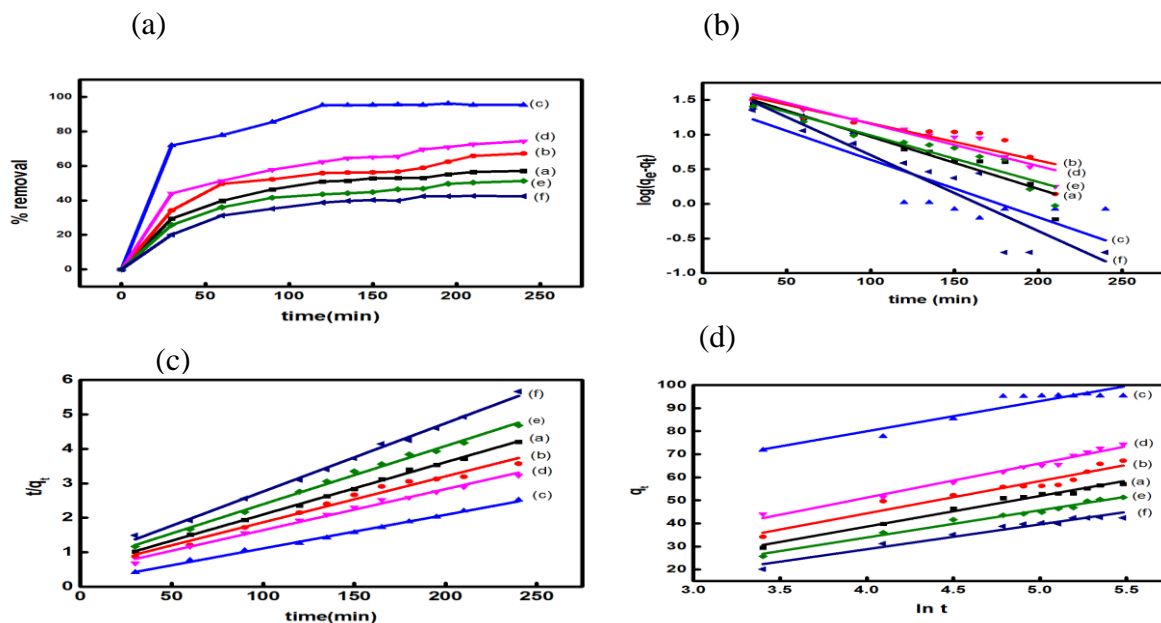


**Fig.5.** (a) Effect of the time on adsorption of CR with initial concentration 100ppm at pH=2, (b) Pseudo-first-order kinetic model, (c) Pseudo-second-order kinetic model, and (d) Elovich model over (a)AL-MIL53 (Al) ,(b) 15wt%,(c) 25wt%,(d) 30wt% ,(e) 50wt%,(f) 60wt% SA- MIL53 (Al) dried at 100 °C

**Table2.** Kinetics for the adsorption of CR (100ppm) at different samples of SA-MIL-53(AL)Sample

	$q_{e,exp}$	Pseudo –first order			Pseudo second order			Elovich equation		
		$q_{ecal}$	$R^2$	$k(\text{min}^{-1})$	$q_{ecal}$	$k \times 10^{-3}$	$R^2(\text{g/mg.min})$	$\alpha$	$\beta$	$R^2(\text{mg/g min})(\text{g/mg})$
AL-MIL53	57.09	52.83	0.87	0.017	65.87	0.39	0.99	0.025	13.28	0.98
15%SAAIMIL3	67.19	50.15	0.71	0.012	75.01	0.33	0.98	0.031	14	0.92
25%SAAIMIL3	96.18	29.5	0.70	0.019	102.45	0.7	0.99	0.629	13.08	0.88
30%SAAIMIL3	74.34	57.97	0.89	0.014	83.89	0.31	0.99	0.038	14.83	0.97
50%SAAIMIL3	51.26	46.02	0.86	0.015	59.13	0.40	0.99	0.027	11.80	0.98
60%SAAIMIL3	42.40	63.46	0.83	0.025	50.47	0.50	0.99	0.024	10.78	0.95

#### 4. Conclusion

This search shows that 25%SA-Al-MIL-53 give the maximum amount of adsorption of CR and the % removal increases with increasing time till reach to equilibrium after 4 h. the maximum amount of adsorption occurs at pH =2. The % removal of CR

increases with increasing dose of adsorbent from 0.03 g to 0.07 then become almost constant from 0.07g to 0.1 g. The kinetics data and adsorption isotherms data show that pseudo

second order and Langmuir isotherm fit for the adsorption of CR.

summarized in Table 2. It is observed that the pseudo 1st order was not describe the adsorption due to the difference in calculated  $q_e$  and experimental  $q_e$ . On the other hand for the Elovich model, the values of  $R^2$  are less than the value of  $R^2$  for pseudo second order so the better kinetic for adsorption is pseudo second order.

second order and Langmuir isotherm fit for the adsorption of CR.

#### 4. References

- 1 X. Cheng, A. Zhang, K. Hou, M. Liu, Y. Wang, C. Song, G. Zhang, X. Guo, (2013) Size- and morphology-controlled NH<sub>2</sub>-MIL-53(Al) prepared in DMF-water mixed solvents, Dalt. Trans. 42 13698–13705. doi:10.1039/c3dt51322j.
- 2 H.K.C. O. M. Yaghi, M. O’Keeffe, N. W. Ockwig, M.E. and J. Kim, No Title,

- (2003) *Nature*. 423 705–714.
- 3 S. Jiang, J. Yan, F. Habimana, S. Ji, (2016) Preparation of magnetically recyclable MIL-53(Al)@SiO<sub>2</sub>@Fe<sub>3</sub>O<sub>4</sub> catalysts and their catalytic performance for Friedel-Crafts acylation reaction, *Catal. Today*. 264 83–90. doi:10.1016/j.cattod.2015.10.003.
  - 4 D.J. Tranchemontagne, J.R. Hunt, O.M. Yaghi, (2008) Room temperature synthesis of metal-organic frameworks: MOF-5, MOF-74, MOF-177, MOF-199, and IRMOF-0, *Tetrahedron*. 64 8553–8557. doi:10.1016/j.tet.2008.06.036.
  - 5 Design and synthesis of an exceptionally stable and highly, 402 (1999) 276–279.
  - 6 R.S. Salama, S.E. Samra, A.I. Ahmed, Adsorption, (2018). Equilibrium and Kinetic Studies on the Removal of Methyl Orange Dye from Aqueous Solution by Using of Copper Metal Organic Framework (Cu-BDC),
  - 7 Y. Zhang, X. Yang, H.C. Zhou, (2018) Synthesis of MOFs for heterogeneous catalysis via linker design, *Polyhedron*. 154 189–201. doi:10.1016/j.poly.2018.07.021.
  - 8 A.G. Wong-foy, A.J. Matzger, O.M. Yaghi, (2010) Ja058213H.Pdf, 3494–3495.
  - 9 C.E. Wilmer, O.K. Farha, T. Yildirim, I. Eryazici, V. Krungleviciute, A.A. Sarjeant, R.Q. Snurr, J.T. Hupp, Gram-scale, (2013) high-yield synthesis of a robust metal-organic framework for storing methane and other gases, *Energy Environ. Sci*. 6 1158–1163. doi:10.1039/c3ee24506c.
  - 10 S. Dhaka, R. Kumar, A. Deep, M.B. Kurade, S.W. Ji, B.H. Jeon, (2019) Metal-organic frameworks (MOFs) for the removal of emerging contaminants from aquatic environments, *Coord. Chem. Rev*. 380 330–352. doi:10.1016/j.ccr.2018.10.003.
  - 11 N.A. Khan, Z. Hasan, S.H. Jung, (2013) Adsorptive removal of hazardous materials using metal-organic frameworks (MOFs): A review, *J. Hazard. Mater*. 244–245 444–456. doi:10.1016/j.jhazmat.2012.11.011.
  - 12 B. Van De Voorde, B. Bueken, J. Denayer, D. De Vos, (2014) Adsorptive separation on metal-organic frameworks in the liquid phase, *Chem. Soc. Rev*. 43 5766–5788. doi:10.1039/c4cs00006d.
  - 13 S.S. Nagarkar, B. Joarder, A.K. Chaudhari, S. Mukherjee, S.K. Ghosh, (2013) Highly selective detection of nitro explosives by a luminescent metal-organic framework, *Angew. Chemie - Int. Ed*. 52 2881–2885. doi:10.1002/anie.201208885.
  - 14 J. Liu, L. Chen, H. Cui, J. Zhang, L. Zhang, C.Y. Su, (2014) Applications of metal-organic frameworks in heterogeneous supramolecular catalysis, *Chem. Soc. Rev*. 43 6011–6061. doi:10.1039/c4cs00094c.
  - 15 P. Ramaswamy, N.E. Wong, G.K.H. Shimizu, (2014) MOFs as proton conductors-challenges and opportunities, *Chem. Soc. Rev*. 43 5913–5932. doi:10.1039/c4cs00093e.
  - 16 C.C. Wang, J.R. Li, X.L. Lv, Y.Q. Zhang, G. Guo, (2014) Photocatalytic organic pollutants degradation in metal-organic frameworks, *Energy Environ. Sci*. 7 2831–2867. doi:10.1039/c4ee01299b.
  - 17 Y. Chen, S. Ma, (2016) Biomimetic catalysis of metal-organic frameworks, *Dalt. Trans*. 45 9744–9753. doi:10.1039/c6dt00325g.
  - 18 Y.R. Lee, J. Kim, W.S. Ahn, (2013) Synthesis of metal-organic frameworks: A mini review, *Korean J. Chem. Eng*. 30 1667–1680. doi:10.1007/s11814-013-0140-6.
  - 19 A. Martinez Joaristi, J. Juan-Alcañiz, P. Serra-Crespo, F. Kapteijn, J. Gascon, (2012) Electrochemical Synthesis of Some Archetypical Zn<sup>2+</sup>, Cu<sup>2+</sup>, and Al<sup>3+</sup> Metal Organic Frameworks, *Cryst. Growth Des*. 12 3489–3498. doi:10.1021/cg300552w.
  - 20 E. Burgaz, A. Erciyes, M. Andac, O. Andac, (2019) Synthesis and characterization of nano-sized metal organic framework-5 (MOF-5) by using consecutive combination of ultrasound and microwave irradiation methods, *Inorganica Chim. Acta*. 485 118–124. doi:10.1016/j.ica.2018.10.014.
  - 21 Z. Jia, M. Jiang, G. Wu, Amino-MIL-53(Al) (2017) sandwich-structure membranes for adsorption of p-

- nitrophenol from aqueous solutions, *Chem. Eng. J.* **307** 283–290. doi:10.1016/j.cej.2016.08.090.
- 22 A. Taheri, E.G. Babakhani, J. Towfighi, (2017) Methyl mercaptan removal from natural gas using MIL-53(Al), *J. Nat. Gas Sci. Eng.* **38** 272–282. doi:10.1016/j.jngse.2016.12.029.
- 23 S.A. El-Hakam, S.E. Samra, S.M. El-Dafrawy, A.A. Ibrahim, R.S. Salama, A.I. Ahmed, (2018) Synthesis of sulfamic acid supported on Cr-MIL-101 as a heterogeneous acid catalyst and efficient adsorbent for methyl orange dye, *RSC Adv.* **8** 20517–20533. doi:10.1039/c8ra02941e.
- 24 M.M. Mane, D.M. Pore, (2016) Sulfamic acid as energy efficient catalyst for synthesis of fluorphores, 1-H-spiro [isoindoline-1,2'-quinazoline]-3,4'(3'H)-diones, *J. Chem. Sci.* **128** 657–662. doi:10.1007/s12039-016-1047-7.
- 25 J. Fu, Z. Chen, M. Wang, S. Liu, J. Zhang, J. Zhang, R. Han, Q. Xu, (2015) Adsorption of methylene blue by a high-efficiency adsorbent (polydopamine microspheres): Kinetics, isotherm, thermodynamics and mechanism analysis, *Chem. Eng. J.* **259** 53–61. doi:10.1016/j.cej.2014.07.101.
- 26 Q. Li, Y. Luo, B. Hou, Z. Han, (2016) Synthesis and Mechanism of Flocculating-Decolorizing Agent PAD used for Polymer-Sulphonated Drilling Wastewater, *J. Residuals Sci. Technol.* **13** 135–143. doi:10.12783/issn.1544-8053/13/2/7.
- 27 M. Takeda, M. Ikeda, S. Satoh, H. Dansako, T. Wakita, N. Kato, Rab13 (2016) is involved in the entry step of hepatitis C virus infection, *Acta Med. Okayama.* **70** 111–118. doi:10.1002/pen.
- 28 I. Petrinić, N. Bajraktari, C. Hélix-Nielsen, (2015) Membrane technologies for water treatment and reuse in the textile industry, *Adv. Membr. Technol. Water Treat. Mater. Process. Appl.* 537–550. doi:10.1016/B978-1-78242-121-4.00017-4.
- 29 M. Saleem, F. Tanveer, A. Ahmad, S.A. Gilani, (2018) Correlation between shoulder pain and functional disability among nurses, *Rawal Med. J.* **43** 483–485. doi:10.1002/app.
- 30 Z. Wu, X. Yuan, H. Zhong, H. Wang, L. Jiang, G. Zeng, H. Wang, Z. Liu, Y. Li, (2017) Highly efficient adsorption of Congo red in single and binary water with cationic dyes by reduced graphene oxide decorated NH<sub>2</sub>-MIL-68(Al), *J. Mol. Liq.* **247** 215–229. doi:10.1016/j.molliq.2017.09.112.
- 31 S.E. Moradi, S. Dadfarnia, A.M. Haji Shabani, S. Emami, (2015) Removal of congo red from aqueous solution by its sorption onto the metal organic framework MIL-100(Fe): equilibrium, kinetic and thermodynamic studies, *Desalin. Water Treat.* **56** 709–721. doi:10.1080/19443994.2014.947328.
- 32 M. Mubashir, Y.F. Yeong, K.K. Lau, T.L. Chew, J. Norwahyu, (2018) Efficient CO<sub>2</sub>/N<sub>2</sub> and CO<sub>2</sub>/CH<sub>4</sub> separation using NH<sub>2</sub>-MIL-53(Al)/cellulose acetate (CA) mixed matrix membranes, *Sep. Purif. Technol.* **199** 140–151. doi:10.1016/j.seppur.2018.01.038.
- 33 L. Liu, X. Tai, N. Zhang, Q. Meng, C. Xin, (2016) Supported Au/MIL-53(Al): a reusable green solid catalyst for the three-component coupling reaction of aldehyde, alkyne, and amine, *React. Kinet. Mech. Catal.* **119** 335–348. doi:10.1007/s11144-016-1034-5.
- 34 R. Abedini, M. Omidkhan, F. Dorosti, (2014) Highly permeable poly(4-methyl-1-pentyne)/NH<sub>2</sub>-MIL 53 (Al) mixed matrix membrane for CO<sub>2</sub>/CH<sub>4</sub> separation, *RSC Adv.* **4** 36522–36537. doi:10.1039/c4ra07030e.
- 35 E. Rahmani, M. Rahmani, Al-Based MIL-53 Metal Organic Framework (MOF) as (2018) the New Catalyst for Friedel-Crafts Alkylation of Benzene, *Ind. Eng. Chem. Res.* **57** 169–178. doi:10.1021/acs.iecr.7b04206.
- 36 S. Huang, H. Pang, L. Li, S. Jiang, T. Wen, L. Zhuang, B. Hu, X. Wang, (2018) Unexpected ultrafast and high adsorption of U(VI) and Eu(III) from solution using porous Al<sub>2</sub>O<sub>3</sub> microspheres derived from MIL-53, *Chem. Eng. J.* **353** 157–166. doi:10.1016/j.cej.2018.07.129.
- 37 R. Dou, J. Zhang, Y. Chen, S. Feng,

- (2017) High efficiency removal of triclosan by structure-directing agent modified mesoporous MIL-53(Al), *Environ. Sci. Pollut. Res.* **24** 8778–8789. doi:10.1007/s11356-017-8583-7.
- 38 B. Brahmaji, S. Rajyalakshmi, T.K. Visweswara Rao, S.R. Valluru, S.K. Esub Basha, C. Satyakamal, V. Veeraiah, K. Ramachandra Rao, (2018) Tb<sup>3+</sup>-added sulfamic acid single crystals with optimal photoluminescence properties for optoelectric devices, *J. Sci. Adv. Mater. Devices.* **3** 68–76. doi:10.1016/j.jsamd.2017.12.002.
- 39 D. Pathania, A. Sharma, Z.M. Siddiqi, (2016) Removal of congo red dye from aqueous system using Phoenix dactylifera seeds, *J. Mol. Liq.* **219** 359–367. doi:10.1016/j.molliq.2016.03.020.
- 40 S. Yan, M. Wang, Y. Zhu, Y. Wu, B. Yi, Q. Yuan, (2018) Removal of methylene blue from aqueous solution by cattle manure-derived low temperature biochar, *RSC Adv.* **8** 19917–19929. doi:10.1039/c8ra03018a.
- 41 X. Cheng, A. Zhang, K. Hou, M. Liu, Y. Wang, C. Song, G. Zhang, X. Guo, (2013) Size- and morphology-controlled NH<sub>2</sub>-MIL-53(Al) prepared in DMF-water mixed solvents, *Dalt. Trans.* **42** 13698–13705.
- 42 H.K.C. O. M. Yaghi, M. O’Keeffe, N. W. Ockwig, *M.E. and*(2003) *J. Kim*, No Title, *Nature.* **423** 705–714.
- 43 S. Jiang, J. Yan, F. Habimana, S. Ji, (2016) Preparation of magnetically recyclable MIL-53(Al)@SiO<sub>2</sub>@Fe<sub>3</sub>O<sub>4</sub> catalysts and their catalytic performance for Friedel-Crafts acylation reaction, *Catal. Today.* **264** 83–90.
- 44 R.S. Salama, S.E. Samra, A.I. Ahmed, *Adsorption* , (2018).Equilibrium and Kinetic Studies on the Removal of Methyl Orange Dye from Aqueous Solution by Using of Copper Metal Organic Framework ( Cu-BDC ),
- 45 Y. Zhang, X. Yang, H.C. Zhou, (2018) Synthesis of MOFs for heterogeneous catalysis via linker design, *Polyhedron.* **154** 189–201.
- 46 A.G. Wong-foy, A.J. Matzger, O.M. Yaghi, (2010) Ja058213H.Pdf, 3494–3495.
- C.E. Wilmer, O.K. Farha, T. Yildirim, I. Eryazici, V. Krungleviciute, A.A. Sarjeant, R.Q. Snurr, J.T. Hupp, Gram-scale, (2013) high-yield synthesis of a robust metal-organic framework for storing methane and other gases, *Energy Environ. Sci.* **6** 1158–1163.
- 48 S. Dhaka, R. Kumar, A. Deep, M.B. Kurade, S.W. Ji, B.H. Jeon, (2019) Metal-organic frameworks (MOFs) for the removal of emerging contaminants from aquatic environments, *Coord. Chem. Rev.* **380** 330–352.
- 49 N.A. Khan, Z. Hasan, S.H. Jung, (2013) Adsorptive removal of hazardous materials using metal-organic frameworks (MOFs): A review, *J. Hazard. Mater.* **244–245** 444–456.
- 50 B. Van De Voorde, B. Bueken, J. Denayer, D. De Vos, (2014) Adsorptive separation on metal-organic frameworks in the liquid phase, *Chem. Soc. Rev.* **43** 5766–5788.
- 51 S.S. Nagarkar, B. Joarder, A.K. Chaudhari, S. Mukherjee, S.K. Ghosh, (2013) Highly selective detection of nitro explosives by a luminescent metal-organic framework, *Angew. Chemie - Int. Ed.* **52** 2881–2885.
- 52 J. Liu, L. Chen, H. Cui, J. Zhang, L. Zhang, C.Y. Su, (2014) Applications of metal-organic frameworks in heterogeneous supramolecular catalysis, *Chem. Soc. Rev.* **43** 6011–6061.
- 53 P. Ramaswamy, N.E. Wong, G.K.H. Shimizu, (2014) MOFs as proton conductors-challenges and opportunities, *Chem. Soc. Rev.* **43** 5913–5932.
- 54 C.C. Wang, J.R. Li, X.L. Lv, Y.Q. Zhang, G. Guo, (2014) Photocatalytic organic pollutants degradation in metal-organic frameworks, *Energy Environ. Sci.* **7** 2831–2867.
- 55 Y. Chen, S. Ma, (2016) Biomimetic catalysis of metal-organic frameworks, *Dalt. Trans.* **45** 9744–9753.
- 56 D.J. Tranchemontagne, J.R. Hunt, O.M. Yaghi, (2008) Room temperature synthesis of metal-organic frameworks: MOF-5, MOF-74, MOF-177, MOF-199,

- and IRMOF-0, *Tetrahedron*. **64** 8553–8557.
- 57 Y.R. Lee, J. Kim, W.S. Ahn, (2013) Synthesis of metal-organic frameworks: A mini review, *Korean J. Chem. Eng.* **30** 1667–1680.
- 58 A. Martinez Joaristi, J. Juan-Alcañiz, P. Serra-Crespo, F. Kapteijn, J. Gascon, (2012) Electrochemical Synthesis of Some Archetypical Zn<sup>2+</sup>, Cu<sup>2+</sup>, and Al<sup>3+</sup> Metal Organic Frameworks, *Cryst. Growth Des.* **12** 3489–3498.
- 59 E. Burgaz, A. Erciyas, M. Andac, O. Andac, (2019) Synthesis and characterization of nano-sized metal organic framework-5 (MOF-5) by using consecutive combination of ultrasound and microwave irradiation methods, *Inorganica Chim. Acta.* **485** 118–124.
- 60 Z. Jia, M. Jiang, G. Wu, Amino-MIL-53(Al) (2017) sandwich-structure membranes for adsorption of p-nitrophenol from aqueous solutions, *Chem. Eng. J.* **307** 283–290.
- 61 A. Taheri, E.G. Babakhani, J. Towfighi, (2017) Methyl mercaptan removal from natural gas using MIL-53(Al), *J. Nat. Gas Sci. Eng.* **38** 272–282.
- 62 S.A. El-Hakam, S.E. Samra, S.M. El-Dafrawy, A.A. Ibrahim, R.S. Salama, A.I. Ahmed, (2018) Synthesis of sulfamic acid supported on Cr-MIL-101 as a heterogeneous acid catalyst and efficient adsorbent for methyl orange dye, *RSC Adv.* **8** 20517–20533.
- 63 R.S. Daries Bella, S. Karthickprabhu, A. Maheswaran, C. Amibika, G. Hirankumar, P. Devaraj, (2015) Investigation of the ionic conductivity and dielectric measurements of poly (N-vinyl pyrrolidone)-sulfamic acid polymer complexes, *Phys. B Condens. Matter.* **458** 51–57.
- 64 M.M. Mane, D.M. Pore, (2016) Sulfamic acid as energy efficient catalyst for synthesis of fluorphores, 1-H-spiro [isoindoline-1,2'-quinazoline]-3,4'(3'H)-diones, *J. Chem. Sci.* **128** 657–662.
- 65 J. Fu, Z. Chen, M. Wang, S. Liu, J. Zhang, J. Zhang, R. Han, Q. Xu, (2015) Adsorption of methylene blue by a high-efficiency adsorbent (polydopamine microspheres): Kinetics, isotherm, thermodynamics and mechanism analysis, *Chem. Eng. J.* **259** 53–61.
- 66 Q. Li, Y. Luo, B. Hou, Z. Han, (2016) Synthesis and Mechanism of Flocculating-Decolorizing Agent PAD used for Polymer-Sulphonated Drilling Wastewater, *J. Residuals Sci. Technol.* **13** 135–143.
- 67 M. Takeda, M. Ikeda, S. Satoh, H. Dansako, T. Wakita, N. Kato, Rab13 is (2016) involved in the entry step of hepatitis C virus infection, *Acta Med. Okayama.* **70** 111–118.
- 68 I. Petrinić, N. Bajraktari, C. Hélix-Nielsen, (2015) Membrane technologies for water treatment and reuse in the textile industry, *Adv. Membr. Technol. Water Treat. Mater. Process. Appl.* 537–550.
- 69 M. Saleem, F. Tanveer, A. Ahmad, S.A. Gilani, (2018) Correlation between shoulder pain and functional disability among nurses, *Rawal Med. J.* **43** 483–485.
- 70 Z. Wu, X. Yuan, H. Zhong, H. Wang, L. Jiang, G. Zeng, H. Wang, Z. Liu, Y. Li, (2017) Highly efficient adsorption of Congo red in single and binary water with cationic dyes by reduced graphene oxide decorated NH<sub>2</sub>-MIL-68(Al), *J. Mol. Liq.* **247** 215–229.
- 71 S.E. Moradi, S. Dadfarnia, A.M. Haji Shabani, S. Emami, (2015) Removal of congo red from aqueous solution by its sorption onto the metal organic framework MIL-100(Fe): equilibrium, kinetic and thermodynamic studies, *Desalin. Water Treat.* **56** 709–721.
- 72 T. Sun, X. Ren, J. Hu, S. Wang, (2014). Supporting Information Expanding Pore Size of Al-BDC MOFs as a Way to Achieve High Adsorption Selectivity for CO<sub>2</sub>/CH<sub>4</sub> Separation,
- 73 M. Mubashir, Y.F. Yeong, K.K. Lau, T.L. Chew, J. Norwahyu, (2018) Efficient CO<sub>2</sub>/N<sub>2</sub> and CO<sub>2</sub>/CH<sub>4</sub> separation using NH<sub>2</sub>-MIL-53(Al)/cellulose acetate (CA) mixed matrix membranes, *Sep. Purif. Technol.* **199** 140–151.
- 74 L. Liu, X. Tai, N. Zhang, Q. Meng, C. Xin, (2016) Supported Au/MIL-53(Al): a reusable green solid catalyst for the three-component coupling reaction of aldehyde,

- 
- alkyne, and amine, *React. Kinet. Mech. Catal.* **119** 335–348.
- 75 R. Abedini, M. Omidkhah, F. Dorosti, (2014) Highly permeable poly(4-methyl-1-pentyne)/NH<sub>2</sub>-MIL 53 (Al) mixed matrix membrane for CO<sub>2</sub>/CH<sub>4</sub> separation, *RSC Adv.* **4** 36522–36537.
- 76 E. Rahmani, M. Rahmani, Al-Based MIL-53 Metal Organic Framework (MOF) as (2018) the New Catalyst for Friedel-Crafts Alkylation of Benzene, *Ind. Eng. Chem. Res.* **57** 169–178.
- 77 S. Huang, H. Pang, L. Li, S. Jiang, T. Wen, L. Zhuang, B. Hu, X. Wang, (2018) Unexpected ultrafast and high adsorption of U(VI) and Eu(III) from solution using porous Al<sub>2</sub>O<sub>3</sub> microspheres derived from IL-53, *Chem. Eng. J.* **353** 157–166.
- 78 R. Dou, J. Zhang, Y. Chen, S. Feng, (2017) High efficiency removal of triclosan by structure-directing agent modified mesoporous MIL-53(Al), *Environ. Sci. Pollut. Res.* **24** 8778–8789.
- 79 B. Brahmaji, S. Rajyalakshmi, T.K. Visweswara Rao, S.R. Valluru, S.K. Esub Basha, C. Satyakamal, V. Veeraiah, K. Ramachandra Rao, (2018) Tb<sup>3+</sup> added sulfamic acid single crystals with optimal photoluminescence properties for optoelectric devices, *J. Sci. Adv. Mater. Devices.* **3** 68–76.
- 80 S. Yan, M. Wang, Y. Zhu, Y. Wu, B. Yi, Q. Yuan, (2018) Removal of methylene blue from aqueous solution by cattle manure-derived low temperature biochar, *RSC Adv.* **8** 19917–19929.